

WEEP: A method for spatial interpretation of weakly supervised CNN models in computational pathology

Abhinav Sharma¹, Bojing Liu¹, Mattias Rantalainen^{1*}

¹ Department of Medical Epidemiology and Biostatistics, Karolinska Institutet, 17165, Sweden

* corresponding author: mattias.rantalainen@ki.se

Abstract

Background

Deep learning enables the modelling of high-resolution histopathology whole-slide images (WSI). Weakly supervised learning of tile-level data is typically applied for tasks where labels only exist on the patient or WSI level (e.g. patient outcomes or histological grading). In this context, there is a need for improved spatial interpretability of predictions from such models.

Results

We propose a novel method, Wsi rEgion sElection aPproach (WEEP), for model interpretation. It provides a principled yet straightforward way to establish the spatial area of WSI required for assigning a particular prediction label. We demonstrate WEEP on a binary classification task in the area of breast cancer computational pathology.

Conclusion

WEEP is easy to implement, is directly connected to the model-based decision process, and offers information relevant to both research and diagnostic applications.

Keywords

Deep learning, Image analysis, Computation pathology, Weakly supervised learning, Spatial Interpretability

Background

Deep learning-based models have demonstrated high performance in a range of prediction tasks in the digital pathology domain. Due to hardware constraints, a common strategy is to divide the gigapixel-size whole slide images (WSIs) into smaller patches (i.e. tiles), which are subsequently modelled by e.g. deep Convolutional Neural Network (CNN) models (1–3). In situations where labels are only available on the WSI level, either due to the absence of pixel-level annotations or the presence of labels exclusively on the WSI level (e.g. patient outcomes), weakly supervised learning is often applied in the domain of computational pathology (4).

Weakly supervised learning has demonstrated broad success in computational pathology, also in the presence of label noise. However, the interpretation of these models is not straightforward, despite the importance of the interpretation in both research applications and clinical decision support applications. Conventional tools for the interpretation of deep CNN models, such as class activation maps (CAM) (5) and Gradient-weighted class activation maps (Grad-CAM) (6), are focused on pixel-level local interpretability (within tile), which do not have a direct interpretation with respect to the predicted label at the WSI level (across all tiles). Recently, trainable attention-based neural networks (7) have been introduced in histopathology image analysis (8). However, the attention weights lack a direct relationship to the decision problem and can therefore not directly be used for determining the set of tiles (i.e. area) required for a particular classification label.

Spatial interpretability has the potential to highlight areas (at tile level) with the most relevant tissue morphology for the particular modelling task at hand. Especially in the context of weakly supervised CNN models of tile-level data, methodology for spatial interpretability linked to the prediction problem has not been available.

To address this problem we propose a novel methodology, the Wsi rEgion sElection aPproach (WEEP), enabling ascertainment of WSI regions that are required for a positive classification label at the slide-level, in the common scenario of tile-based weakly supervised learning. The approach is easy to implement and has a direct interpretation with respect to the prediction problem, and is therefore relevant in both research and clinical application contexts. We describe the methodology and apply it to identify classification-essential WSI regions from two different tile-to-slide level aggregation functions: a trivial mapping function based on the 75th percentile of tile-level prediction scores from CNN models, and a tile-level attention scores from a trainable attention-based pooling layer. To illustrate the method, we apply it to a binary classification task that distinguishes histological grade 1 and 3 in breast cancer.

Methods

WEEP method description

Multiple Instance learning (MIL) is one of the standard frameworks for weakly supervised learning problems in computational pathology (9). In a standard MIL framework, a bag (represented by the WSI) contains instances (represented by the tiles), and if at least one of the instances is classified as positive then the whole bag is classified as positive. However, in real-world computational pathology applications, the bag level label is typically assigned based on a function that accounts for more than a single tile in order to achieve optimal prediction performance. The MIL framework can be divided into two steps: first, the

tile-level feature representations/prediction scores are obtained from a base CNN model and second: these feature representations/prediction scores are aggregated to provide the WSI prediction score using a tile-to-slide aggregator function or model. Different tile-to-slide level aggregator functions have been used in different weakly supervised classification scenarios (10).

WEEP exploits a fundamental property of MIL models applied to tile-level instances of the histopathology WSIs. Specifically, we assume the existence of a model that provides tile-level predictions, that allow the ranking of tiles with respect to the prediction task, based on e.g. predicted class probabilities, such that two instances x_i and x_j , $p(\text{class}=1 | x_i) > p(\text{class}=1 | x_j)$ implies x_i is more likely than x_j to belong to class 1, conditional upon the model and the tile. In the case of a simple tile-to-slide mapping function, e.g. mean, median or 75-percentile, of the tile distribution, we can simply use the tile class probability prediction. However, in cases where we have a second trainable model for slide-level predictions that has attention weights, these weights can also be considered as the ranking metric.

Irrespective of the ranking metric, a backward selection approach can be applied, which provides guarantees that the selected subset is the maximum set of tiles needed for positive classification on the WSI level. Backward selection is a common strategy that has been used for variable selection in predictive modelling tasks (11). Here, we apply it to identify the set of instances (tiles) required for a positive classification label (Table 1). In our empirical evaluation results, we consider tile-level predicted class probability as well as attention weights as ranking metrics. The WEEP algorithm allows us to determine the set of tiles directly required to assign the WSI label.

```

1. for a model  $M$ ; and a WSI with a set of  $x$  tiles:
2.    $x_{\text{selected}} = \{\}$ 
3.   sort the set of tiles  $x$ , based on  $p(\text{NHG}=3 \mid x_i)$ , or
     attention weights ( $a_i$ ) in descending order
4.   calculate the slide-level prediction score,  $P = f(x, M)$ 
5.   while  $P \geq O$ :
6.      $x_{\text{selected}} = x_{\text{selected}} \cup \{x_i\}$  (store the selected tile)
7.      $x = x \setminus x_i$  (remove the selected tile from the set)
8.     update the slide-level prediction score,  $P = f(x, M)$ 
9.    $x_{\text{selected}}$  is the set of tiles that constitute the
     tiles/region driving the classification of the WSI

```

Table 1: Outline of the steps in the WEEP algorithm. (O represents the established decision threshold)

Study materials

In this study, we included patients from the SöS-BC-4 cohort, collected from the Södersjukhuset (South General Hospital) in Stockholm, Sweden from the year 2012-2018. One Hematoxylin and Eosin (H&E) stained WSI scanned at 40X magnification level was considered from each patient. WSI preprocessing steps were followed as described in (12). We only included tiles predicted as invasive cancer (tile size: 598x598 pixels) in further analyses.

The models were optimised and validated on the training set ($n = 1695$) using 5-fold cross-validation (cv). The training set was split into CV training and CV test set for each cv fold. Further, the CV training set was split into the feature extractor training set, attention module training set, and the tuning set as defined in (13). Each data split was stratified by the clinical NHG.

Optimisation of the CNN model and the trainable attention model

We considered the Resnet-18 CNN model architecture (14) as the tile-level classification model and as the feature extractor for the attention module. Pretrained model from Imagenet

was used to initialise the model weights (15) and was fine-tuned on the feature extractor training set as the binary histological grade 1 vs 3 classification model.

The tile-level feature vectors were extracted from the average pooling layer of the CNN models for tiles in the attention module training set and tuning set. The attention layer is a trainable layer inspired by (9), which optimises an attention weight to each tile-level feature vector and provides a slide-level prediction score by performing a weighted average of all tile-feature vectors belonging to that slide. The tuning set was used to monitor the model learning curves and selection of the best model according to the early stopping criteria used for both CNN and the attention model. The early stopping criteria was defined as no improvement in tuning loss for the consecutive 50 partial epochs (patience). The attention module was optimised as the binary classification model to classify NHG 1 vs 3.

Validation on the CV test set

The optimised CNN model and the attention model were validated on the CV test set in each CV fold. The 75th percentile of the tile-level prediction scores from the CNN model was used to provide the slide-level prediction score as the first aggregation function (12). The second aggregation function consisted of the attention model to provide the slide-level prediction scores from the tile-level feature vectors extracted from the CNN model. We further aggregated the slide-level prediction scores from the five CV test sets and evaluated the optimal classification threshold to classify the WSIs as Grade 3 and 1 using Youden's statistics.

Quantitative and Visual analysis of selected regions in different modelling strategies

We considered the assessment of the WSI regions contributing to the classification of the histological grade 3 WSIs ($n = 543$). We demonstrated the iterative backward selection approach of the WEEP methodology as the line plot (referred to as the *WEEP plot*). Further, we observed the distribution of the percentage of selected tiles for each WSI in the CV test set using the histogram plots. The selected tiles using WEEP for the example WSIs were visualised over the tumour mask on the low-resolution WSI as the binary mask. All the plots were created using the package matplotlib (v.3.6.2) (16) in python (v.3.10.8).

Results

Evaluating the selected regions from different modelling strategies

First, we applied WEEP to analyse two different tile-to-slide aggregation functions for the binary classification problem of NHG 1 vs 3, and visualised the results as the WEEP plot (Figure 1a, 1c). The results reveal the trajectories of the WEEP backward selection and the corresponding WSI-level prediction score, the horizontal line shows the decision boundary established on the full dataset. Next, we investigated the distribution of the proportion of tiles that were selected by WEEP in each WSI (Figure 1b, 1d). For the ResNet-18 model with 75th percentile tile-to-slide aggregator function, a mean percentage of 32.34% (95% CI: 29.69% - 34.99%) was observed as the average percentage of tiles contributing to the histological grade 3 classification in each slide. For the ResNet-18 model

with the attention module, we observed the mean percentage of selected tiles as 44.97% (95% CI: 41.69% - 48.26%).

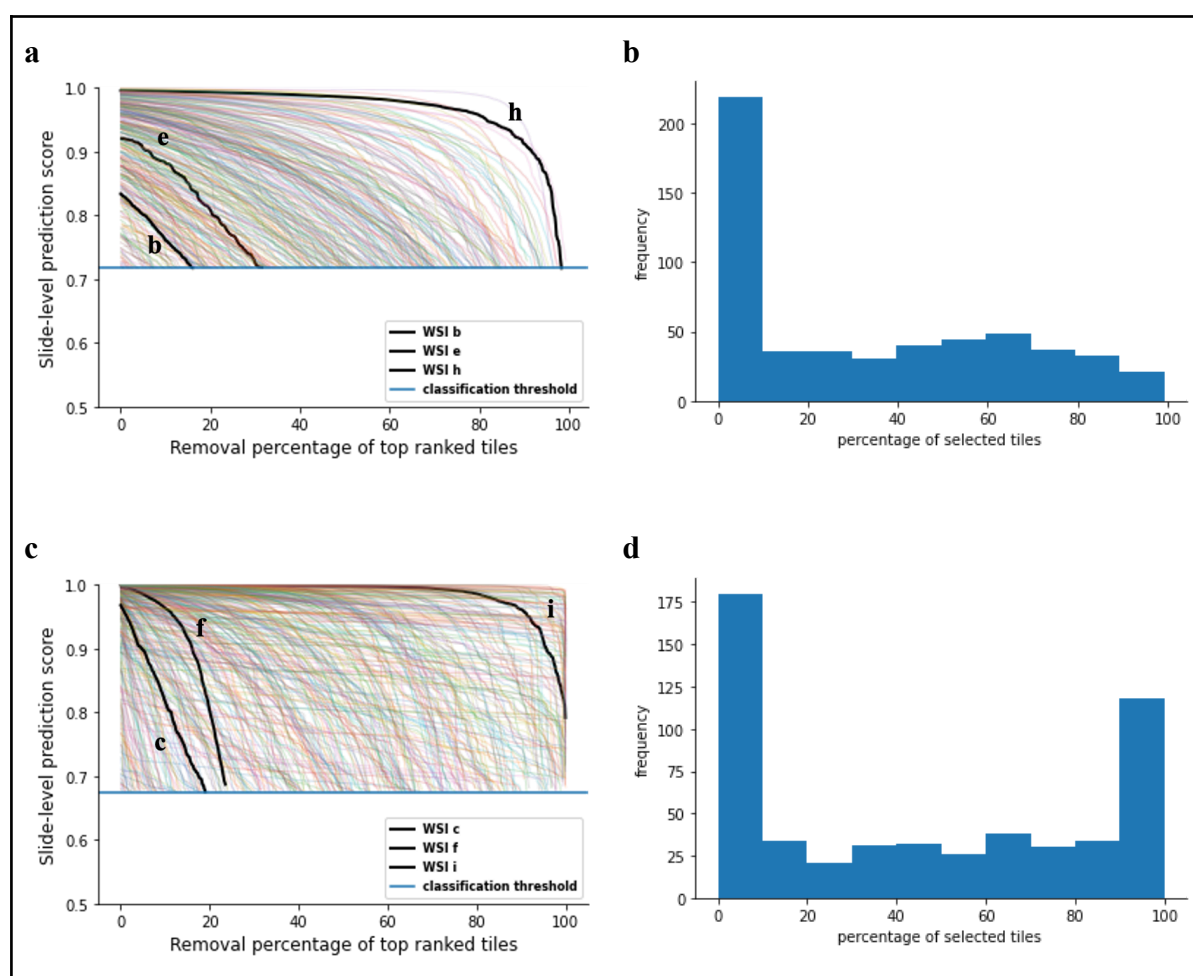


Figure 1: Application of WEEP to a binary classification problem. We have randomly selected and highlighted three clinical NHG 3 WSIs with each WSI randomly selected from the ranges $<20\%$, $>20\%$ & $<80\%$ and $>80\%$ of the selected tiles through WEEP respectively. They are highlighted (black) in plots **a**, **c** and marked by the plot labels of Figure 2. **a** WEEP plot showing the change in slide-level prediction score with the step-wise backward removal of top-ranked tiles until the slide-level prediction score reaches the classification threshold, here the ranking of the tiles was based on tile-level prediction scores and slide level score was determined using 75th percentile

tile-to-slide aggregation function. **b** Distribution of the percentage of selected tiles for each WSI from the backward selection approach when applied to the ResNet-18 model with 75th percentile tile-to-slide aggregation function. **c** WEEP plot to show the change in slide-level prediction score with the step-wise backward removal of top-ranked tiles, with the ranking based on attention scores from the ResNet-18 model with attention module. **d** Distribution of the percentage of the selected tiles for each WSI when applied to the ResNet-18 model with attention module.

Visualisation of the selected regions from different modelling strategies

To provide an example of the resulting spatial interpretation, we visualised the selected regions for different modelling strategies (Figure 2). Revealing the spatial localization and WSI regions that are directly linked with the classification of histological grade 3 WSIs.

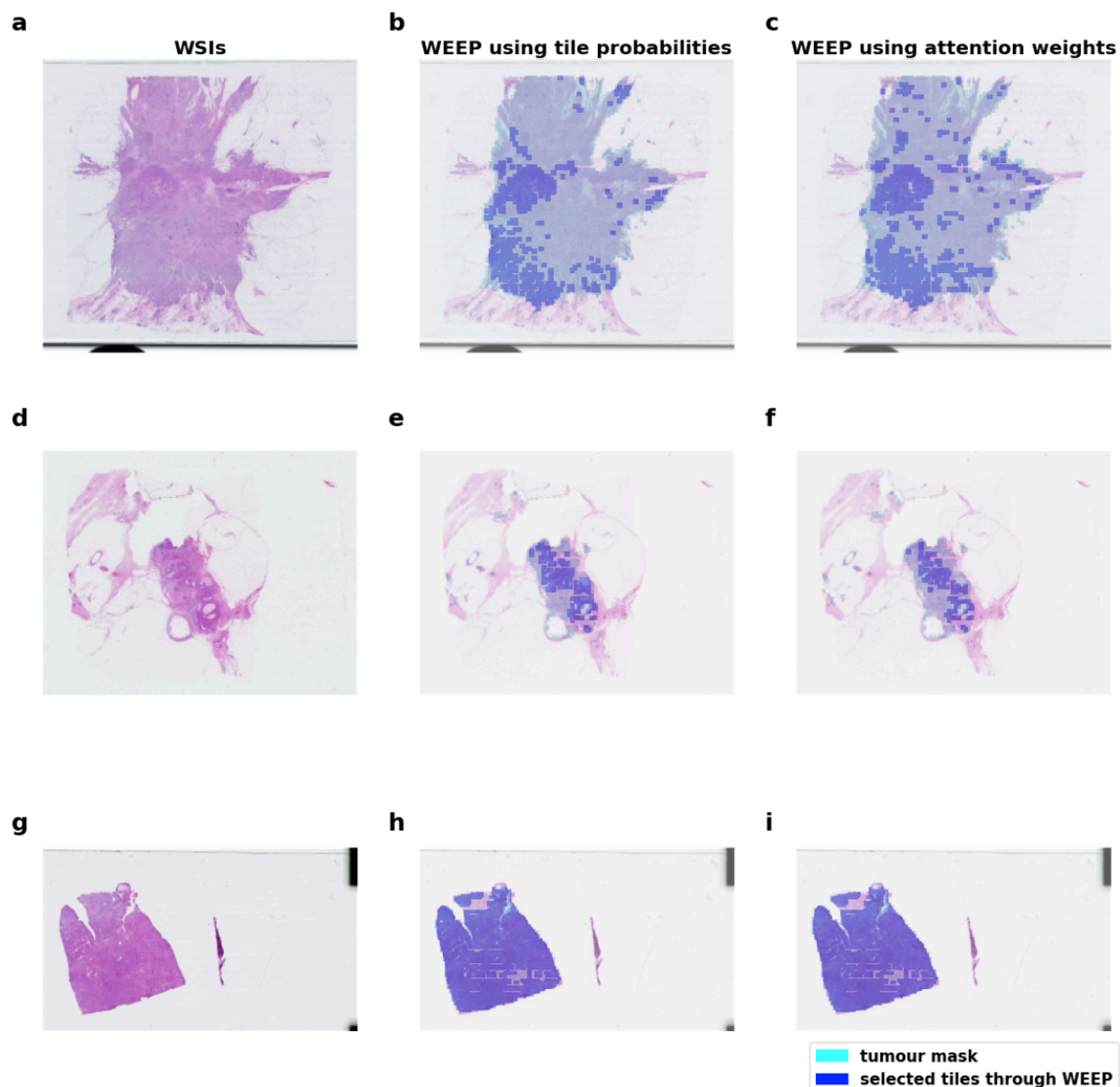


Figure 2: Binary masks of the selected tiles through WEEP over the tumour mask on the original WSI. Randomly selected three clinical NHG 3 WSIs from Figure 1 have been demonstrated here. **b**, **e**, **f** The second column represents the binary masks of the selected tiles by applying WEPP to the tiles ranked by tile-level prediction scores. **c**, **f**, **i** The third column represents the binary masks of the selected tiles by applying WEPP to the tiles ranked by attention scores.

Discussion

In this study, we proposed WEEP, a method that provides a spatial tile-level interpretation of deep learning models for prediction modelling of histopathology whole slide images. WEEP is directly linked to the WSI level prediction by a deep learning model and is based on the ranking of the tile-level predictions together with the application of a backward selection strategy to define the subset of tiles driving the assignment of a classification label.

WEEP was demonstrated on a CNN model to classify histological grade 1 vs 3 in invasive breast cancer patients and evaluated two different tile-to-slide aggregation functions i.e. 75th percentile of the tile level prediction scores and the trainable attention layer. We demonstrated the methodology and visually explored the selected regions in the histological grade 3 patients.

CAM-based approaches are common for pixel-level image interpretation but lack a direct connection to the models' assignment of predictions and decision-making. While the pixel-level information can be of importance to subjectively interpret the model and image patterns learned, areas that are directly linked to how classification labels are assigned are not provided by CAM-based methodologies. Moreover, different CAM-based approaches provide different saliency maps for the same CNN model, which raises questions about the reliability of these methods in offering robust interpretation, especially when semantic pixel-level annotations are not available by definition (e.g. as is the case for prognostic models or other patient outcome-oriented tasks) so that the methods can not be validated by ground truth annotations (17). In our application domain of histopathology images modelled

as tiles, there is also a direct limitation as CAM-based methods only offer interpretability on individual tiles, making it even harder to identify areas (tiles) across multiple instances in a single WSI that are relevant for assignment of the class label (18).

MIL-based methods utilising the tile-level class probabilities to aggregate the WSI-level prediction score are hard to interpret since it is unclear to establish the thresholding on tile-level class probabilities to identify the discriminatory tiles in the WSI. Occlusion Sensitivity Analysis (OSA) have been reported to find discriminatory regions locally (in the tiles) by applying the moving mask in the different regions of the tiles and observing the model's sensitivity (tile-level prediction score) to the different masked regions in a tile (19). It provides an approach for the local interpretability of the selected tiles if needed but does not have a direct association with the WSI-level classification label. Secondary trainable models for tile-to-slide aggregation like the attention-based approach by Lu et al. provide attention weights to directly visualise the highly discriminatory tiles involved in the classification of the WSI (9). However, precise identification of the regions that are needed for the slide-level classification is not possible.

In the specific classification scenario of breast cancer histological grading assessment that includes high inter-observer (20) and inter-lab variability (21), pathologists assign the NHG label on the WSI and it is not possible to obtain well-defined pixel/tile level annotation by definition. To address this problem, multiple MIL-based weakly-supervised CNN-based approaches have been developed especially for the histological grade 1 vs 3 binary classification from the H&E WSIs (12,13,22,23). However, it is important to understand the underlying regions recognised by the models and here, the WEEP methodology can be

potentially beneficial in providing regions of interest that are directly associated with the classification of the WSI.

WEEP has strengths and limitations. One of the main limitations is that the interpretation is provided on the tile level, whereas CAM-based methods are focused on pixel-level interpretations. Secondly, WEEP utilises the underlying model-based ranking of the tiles, which is a potential constraint as the results are conditional upon the model. The major strength lies in the simplicity and empirical approach to defining the direct association of the tiles to the predicted WSI label. The method can also be extended to the multiclass and regression problems. In the multiclass scenario, WEEP can be applied to the tile-level class probabilities of the predicted class the WSI. In the regression objectives, it is possible to apply WEEP until the WSI prediction intersects with the e.g. mean (or median) of the predicted response variable.

Conclusions

The proposed WEEP method provides a direct selection of tiles and regions that could be utilised to visually interpret the decision-making of such tile-based CNN classification models. The selected regions can be studied further to understand different tissue morphologies used by the model for classification and could be used to determine novel morphological patterns or confirm the learning of the existing associated morphologies by the CNN-based model.

List of abbreviations

WSI: Whole Slide Image

CNN: Convolutional Neural Network

CAM: Class Activation Maps

Grad-CAM: Gradient-weighted class activation maps

WEEP: Wsi rEgion sElection aPproach

MIL: Multiple Instance Learning

H&E: Hematoxylin and Eosin

CV: Cross-Validation

OSA: Occlusion Sensitivity Analysis

Declarations

Ethics approval and consent to participate

The study has approval by the regional ethics review board (Stockholm, Sweden)

Consent for publication

Not Applicable

Availability of data and materials:

Data in the study cannot be made publicly available due to legal constraints. Reasonable access requests to the corresponding author will be considered. The implementation of the WEEP methodology is available at: <https://github.com/rantalainenGroup/WEEP>.

Competing interests:

MR is a shareholder of Stratipath AB. All other authors have declared no conflicts of interest.

Funding:

This work was supported by funding from the Swedish Research Council, Swedish Cancer Society, Karolinska Institutet, ERA PerMed (ERAPERMED2019-224-ABCAP), VINNOVA and SweLIFE (SwAIPP project), MedTechLabs, Swedish e-science Research Centre (SeRC) - eCPC, Stockholm Region, Stockholm Cancer Society and Swedish Breast Cancer Association.

Authors' contributions:

AS: Data curation, Formal Analysis, Visualisation, Preparing draft of manuscript, Editing manuscript

BL: Supervision, Preparing draft of manuscript, Editing and approval of manuscript

MR: Conceptualisation, Methodology, Visualisation, Funding acquisition, Supervision, Preparing draft of the manuscript, Editing and approval of manuscript

Acknowledgements:

Not applicable

References:

1. Coudray N, Ocampo PS, Sakellaropoulos T, Narula N, Snuderl M, Fenyo D, et al. Classification and mutation prediction from non-small cell lung cancer histopathology images using deep learning. *Nat Med*. 2018 Oct;24(10):1559–67.
2. Campanella G, Hanna MG, Geneslaw L, Miraflor A, Werneck Krauss Silva V, Busam KJ, et al. Clinical-grade computational pathology using weakly supervised deep learning on whole slide images. *Nat Med*. 2019 Aug;25(8):1301–9.
3. Ström P, Kartasalo K, Olsson H, Solorzano L, Delahunt B, Berney DM, et al. Artificial intelligence for diagnosis and grading of prostate cancer in biopsies: a population-based, diagnostic study. *Lancet Oncol*. 2020 Feb;21(2):222–32.
4. Augustine TN. Weakly-supervised deep learning models in computational pathology. *EBioMedicine*. 2022 Jul;81:104117.
5. Zhou B, Khosla A, Lapedriza A, Oliva A, Torralba A. Learning deep features for discriminative localization. In: 2016 IEEE Conference on Computer Vision and Pattern Recognition (CVPR) [Internet]. IEEE; 2016 [cited 2023 Feb 27]. Available from: http://cnnlocalization.csail.mit.edu/Zhou_Learning_Deep_Features_CVPR_2016_paper.pdf
6. Selvaraju RR, Cogswell M, Das A, Vedantam R, Parikh D, Batra D. Grad-CAM: Visual Explanations from Deep Networks via Gradient-Based Localization. In: 2017 IEEE International Conference on Computer Vision (ICCV). 2017. p. 618–26.
7. Jetley S, Lord NA, Lee N, Torr PHS. Learn To Pay Attention [Internet]. arXiv [cs.CV]. 2018. Available from: <http://arxiv.org/abs/1804.02391>
8. van der Velden BHM, Kuijf HJ, Gilhuijs KGA, Viergever MA. Explainable artificial intelligence (XAI) in deep learning-based medical image analysis. *Med Image Anal*. 2022 Jul;79:102470.
9. Lu MY, Williamson DFK, Chen TY, Chen RJ, Barbieri M, Mahmood F. Data-efficient and weakly supervised computational pathology on whole-slide images. *Nat Biomed Eng*. 2021 Jun;5(6):555–70.
10. Bilal M, Jewsbury R, Wang R, AlGhamdi HM, Asif A, Eastwood M, et al. An aggregation of aggregation methods in computational pathology. *Med Image Anal*. 2023 Aug;88:102885.
11. Déjean S, Ionescu RT, Mothe J, Ullah MZ. Forward and backward feature selection for query performance prediction. In: Proceedings of the 35th Annual ACM Symposium on Applied Computing. New York, NY, USA: Association for Computing Machinery; 2020. p. 690–7. (SAC '20).
12. Wang Y, Acs B, Robertson S, Liu B, Solorzano L, Wahlby C, et al. Improved breast cancer histological grading using deep learning. *Ann Oncol*. 2022 Jan;33(1):89–98.
13. Sharma A, Weitz P, Wang Y, Liu B, Vallon-Christersson J, Hartman J, et al. Development and prognostic validation of a three-level NHG-like deep learning-based model for histological grading of breast cancer. *Breast Cancer Res*. 2024 Jan 29;26(1):17.
14. He K, Zhang X, Ren S, Sun J. Deep Residual Learning for Image Recognition. In: 2016 IEEE Conference on Computer Vision and Pattern Recognition (CVPR). 2016. p. 770–8.
15. Deng J, Dong W, Socher R, Li LJ, Li K, Fei-Fei L. ImageNet: A large-scale hierarchical image database. In: 2009 IEEE Conference on Computer Vision and Pattern Recognition. 2009. p.

248–55.

16. Hunter JD. Matplotlib: A 2D Graphics Environment. *Comput Sci Eng*. May-June 2007;9(3):90–5.
17. Syed S, Anderssen KE, Stormo SK, Kranz M. Weakly supervised semantic segmentation for MRI: exploring the advantages and disadvantages of class activation maps for biological image segmentation with soft boundaries. *Sci Rep*. 2023 Feb 13;13(1):2574.
18. Shao F, Chen L, Shao J, Ji W, Xiao S, Ye L, et al. Deep Learning for Weakly-Supervised Object Detection and Object Localization: A Survey [Internet]. arXiv [cs.CV]. 2021. Available from: <http://arxiv.org/abs/2105.12694>
19. Gallo M, Krajňanský V, Nenutil R, Holub P, Brázdil T. Shedding light on the black box of a neural network used to detect prostate cancer in whole slide images by occlusion-based explainability. *N Biotechnol*. 2023 Oct 2;78:52–67.
20. Ginter PS, Idress R, D'Alfonso TM, Fineberg S, Jaffer S, Sattar AK, et al. Histologic grading of breast carcinoma: a multi-institution study of interobserver variation using virtual microscopy. *Mod Pathol*. 2021 Apr;34(4):701–9.
21. Acs B, Fredriksson I, Rönnlund C, Hagerling C, Ehinger A, Kovács A, et al. Variability in Breast Cancer Biomarker Assessment and the Effect on Oncological Treatment Decisions: A Nationwide 5-Year Population-Based Study. *Cancers* [Internet]. 2021 Mar 9;13(5). Available from: <http://dx.doi.org/10.3390/cancers13051166>
22. Couture HD, Williams LA, Geradts J, Nyante SJ, Butler EN, Marron JS, et al. Image analysis with deep learning to predict breast cancer grade, ER status, histologic subtype, and intrinsic subtype. *NPJ Breast Cancer*. 2018 Sep 3;4:30.
23. Wetstein SC, de Jong VMT, Stathonikos N, Opdam M, Dackus GMHE, Pluim JPW, et al. Deep learning-based breast cancer grading and survival analysis on whole-slide histopathology images. *Sci Rep*. 2022 Sep 6;12(1):15102.